Report on a problem studied at the UK Mathematics-in-Medicine Study Group Oxford 2005
< https://mmsg.mathmos.net/uk/2005/hepatic-lipoproteins/ >

Mathematical Models of Hepatic Lipoprotein Metabolism

Jasmina Panovska, Laura Pickersgill, Marcus Tindall, Jonathan Wattis and Helen Byrne

10th August 2006

Abstract

Two mathematical models of lipoprotein particle metabolism by liver cells (hepatocytes) are formulated. The first model describes low density lipoprotein (LDL) particle uptake using a discrete model formulation and allows differences in the number of free, bound and internalised LDL particles to be elucidated. A second continuum model provides a description of LDL and very low density lipoprotein (VLDL) particle uptake and the competition between the particles for free LDL receptors. Both models provide initial insight into testing biological hypotheses on the competition between LDL and VLDL particle binding and uptake. Comparison with experimental data is made where appropriate and suggestions for further model development are made.

1 Introduction

Mammalian cells have evolved complex mechanisms to transport dietary and endogenous cholesterol via the plasma to tissues and to ensure that cellular accumulation of cholesterol is avoided.

Cholesterol is transported throughout the plasma by a family of macromolecular complexes called lipoproteins. In humans, the majority (approximately two thirds) of plasma cholesterol is found within the low density lipoprotein (LDL) class of lipoproteins. An elevated level of plasma LDL-C is the most widely accepted risk factor for the development of cardiovascular disease. LDL-C levels are in part determined by the rate at which LDL particles are taken up by liver cells (hepatocytes). The uptake of LDL by the liver is highly controlled. The first step in this process involves an LDL particle binding to hepatic LDL receptors (LDLR), in specialised regions of the liver cell plasma membrane known as coated pits. This interaction is mediated by apolipoprotein B (apoB) present on the surface of LDL particles. Upon binding to the LDLR, LDL particles are internalised by endocytosis, forming intracellular vesicles known as endosomes. Fusion of endosomes with lysosomes results in the degradation of the LDL particle into its constituent parts (e.g. cholesterol, fatty acids and amino acids). The LDLRs are either recycled to the cell surface or degraded (see Figure 1(a)-(c)).

The rate at which LDL particles are taken up by the liver is influenced by the presence of other plasma lipoproteins, namely the triglyceride-rich lipoprotein (TRL) which consists of very low density lipoproteins (VLDL) and chylomicrons (CM). The concentration of plasma TRL increases following a fat-containing meal, and these particles are thought to bind to the LDLR

via TRL-associated apolipoprotein E (apoE) molecules, thus competing with LDL for LDLR binding. Recent experimental evidence shows that TRL particles contained within the VLDL fraction (these particles will be referred to as VLDL in the remainder of the report) isolated from individuals following meals rich in mono-unsaturated (MUFA), polyunsaturated (PUFA) and saturated (SAFA) fat differ in their ability to compete with LDL for hepatic uptake, with SAFA-VLDL being better competitors than PUFA-VLDL or MUFA-VLDL. SAFA-VLDL carry more apoE molecules than MUFA-/PUFA-VLDL (an average of 3 and 2 molecules apoE per particle respectively), and when the number of apoE molecules per experiment is normalised, the meal-dependent effects on the inhibition of LDL uptake are no longer apparent. This data suggests that one of the mechanisms by which SAFA-rich diets may lead to elevated LDL-C levels is via the production of apoE-rich particles, which more efficiently compete with LDL for binding to the LDLR.

Many structural and compositional features distinguish LDL and VLDL particles. Firstly LDL particles are much smaller than VLDL particles (see Table 1). Secondly, LDL contains one molecule of apoB alone, whereas VLDL contains one molecule of apoB (probably in a LDLR-inactive form) and multiple copies of apoE. LDL contains approximately 3400 molecules of cholesterol, whereas SAFA-VLDL (VLDL-3) and PUFA-/MUFA-VLDL (VLDL-2) contain 3900 and 3200 molecules of cholesterol respectively

As mentioned above, in the presence of increasing numbers of VLDL particles, LDL uptake by the liver decreases (see Figure 2). Gene expression data gathered in the presence and absence of VLDL would suggest that there is a drop in the intracellular cholesterol concentration in the presence of VLDL, and that this drop is greater in the presence of VLDL-3 than VLDL-2 particles. Two alternative hypotheses (Hyp 1 and Hyp 2) have been postulated to explain these observations:

Hyp 1. VLDL bind non-specifically to proteoglycans on the surface of liver cells via apoE. These particles are not internalised, but rather block a collection of LDLRs, leading to a reduction in the amount of LDL which can access LDLRs and a consequent reduction in intracellular cholesterol levels. This scenario is depicted in Figure 1(b).

Hyp 2. VLDL particles bind to LDLRs via apoE and are subsequently internalised. Since VLDL are larger than LDL and have multiple apoE molecules, each VLDL particle can block the internalisation of several LDL particles, thus leading to a reduction in the total amount of cholesterol molecules entering the cell. This scenario is depicted in Figure 1(c).

In this report we present mathematical models to compare the hypotheses outlined above regarding LDL and VLDL uptake by the liver and the resulting intracellular cholesterol levels. The main challenge is to provide insight into LDL endocytosis, in the presence and absence of VLDL particles.

The particular experiments upon which our mathematical modelling will focus involved exposing liver cells, that had been starved of cholesterol, to a fixed amount of LDL either alone or in the presence of increasing numbers of VLDL particles. These experiments were conducted for a period of five hours to determine the levels of bound and internalised LDL and LDL degradation products. Two different theoretical models of these experiments are presented in this report: in the first model LDL endocytosis in the absence of VLDL is explored whilst in the second model the effects of VLDL uptake are incorporated. In addition, in the first model we focus on the LDL content of the pits on the surface of the cells, assuming that each pit

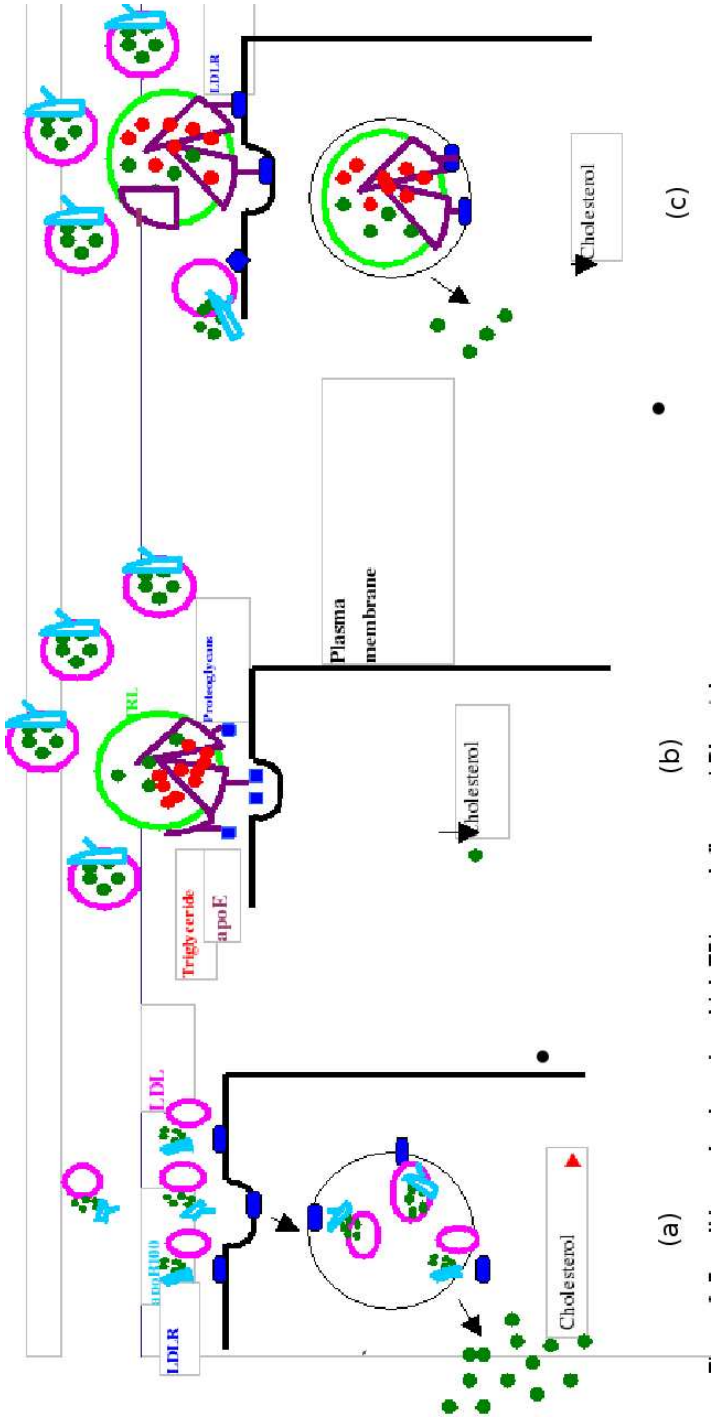

Figure 1: Schematic representation of three different scenarios describing LDL endocytosis in the liver cells. In we depict (a) LDL particle binding, internalisation and digestion occur in the absence of VLDL particles. In (b) LDL and VLDL compete for LDLR binding. VLDL are not taken up by the cell, but their binding reduces the amount of LDL taken up by the cell (this corresponds to Hyp 1). In (c) VLDL bind to the LDLR and are internalised (this corresponds to Hyp 2). This picture is reproduced from [3] with permission.

Description	Value
Number of pits per cell	80
Number of receptors per cell	35,000 (70% in pits)
Number of receptors per pit	$\sim$ 306 (Discrepancy due to only $\sim$ 70% of receptors being located in pits.)
Radius of LDL	10 nm
Number of receptors covered by LDL particle	31
Radius of VLDL particle	15-40nm
Number of receptors covered by VLDL particle	70
Average radius of a pit	200 nm (Range of 15-500nm.)
Length of cell	10 μm

Table 1: Characteristics and properties of an individual liver cell, the LDL particles and the VLDL particles.

has a fixed number of receptors, and that each pit can bind several LDL particles before being internalised. In the second model, we do not explicitly consider the pits, concentrating instead on the receptors on the cell surface and competition between LDL and VLDL for receptors. The aim of this latter model is to account for the reduced cholesterol content of cells in the presence of VLDL particles, in particular VLDL-3. The former case is considered in Section 2 and the latter in Section 3. Our conclusions and suggestions for future research directions are presented in Section 4.

2 LDL endocytosis in the absence of VLDL

2.1 Model development

In this section we study the dynamics of LDL endocytosis. We model the binding and internalisation of LDL particles together with their subsequent conversion to cholesterol within the liver cells. We also allow for cholesterol loss across the cell wall, to the extracellular environment. We derive a system of ordinary differential equations which describe how the physical variables of interest evolve over time. Dimensional quantities will be denoted by barred symbols. In the subsequent subsections we consider parameter values and non-dimensionalise the model.

The biochemistry of LDL endocytosis follows the following steps: we assume that external LDL particles L_e are bound to receptors in a pit on the surface of a hepatocyte. On internalisation of a pit, bound LDL particles L_b are also internalised by the cell; we use L_i to denote internalised LDL particles. Internalised LDL is broken down into cholesterol (C), which can have several metabolic fates. It can be incorporated into cellular membranes, esterified to the C storage form cholesterol ester (CE), or metabolised through oxidation. In summary, we have the reactions

$$L_e \xrightarrow{\overline{a}} L_b \xrightarrow{\overline{b}} L_i \xrightarrow{\overline{k}_{id}} \overline{r}C \xrightarrow{\overline{\lambda}} \{\}, \tag{1}$$

where the quantities $\overline{a}$, $\overline{b}$, $\overline{k}_{id}$, $\overline{\lambda}$ are rates, $\overline{r}$ is the number of cholesterol molecules in a typical LDL particle and denotes the products of cholesterol degredation.

We denote by $\overline{N}_p(t)$ the number of pits with $0 \leq p \leq p_m$ LDL particles bound. Then $\overline{N}_0(t)$ represents the number of pits that are free of LDL at time t and p_m denotes the maximum

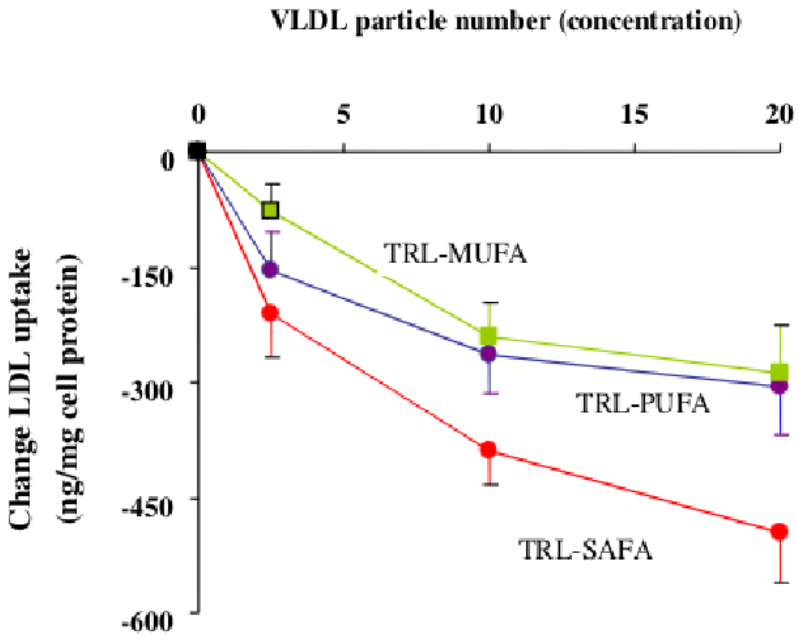

Figure 2: Experimental results how LDL uptake decreases when liver cells are cultured in medium containing a constant concentration of LDL and increasing concentrations of VLDL. Key: medium contains LDL and VLDL enriched in saturated fatty acids (SAFA-VLDL) (red curve); medium contains VLDL enriched in polyunsaturated fatty acids (PUFA-VLDL) (blue line); or, medium contains VLDL enriched in monounsaturated fatty acids (MUFA-VLDL) (green line). This graph is reproduced from [3] with permission.

number of LDL particles that can bind to a coated pit ($0 < p_m < \infty$). Our mathematical model describes how the number of pits containing $0, 1, 2, \ldots, p_m$ LDL particles changes over time. It also describes the evolution of the external concentration of LDL particles ($\overline{L}_e$), the concentrations of bound ($\overline{L}_b$) and internalised ($\overline{L}_i$) LDL particles and cholesterol ($\overline{C}$).

In developing our model, we start by considering how $\overline{N}_0(t)$ evolves. We assume that empty pits are produced at a constant rate $\overline{k}_0$ [1]. LDL may bind to empty pits, and also to pits containing one or more LDL particles. We define this sequential binding of LDL particles iteratively

$$N_{p-1} + L_e \xrightarrow{\overline{a}} N_p + L_b, \quad p = 1, 2, \ldots, p_m. \tag{2}$$

Occupied pits are internalised at a rate $\overline{b}$ and empty ones at a lower rate $\overline{b}_0$.

We use the law of mass action to derive differential equations from the chemical reactions (1)–(2). The equations for $\overline{N}_p(t)$, which are the time-dependent concentrations $[N_p]$ for $p = 1, \ldots, p_m$, have a source term due to LDL binding at rate $\overline{a}$ to a pit with $(p-1)$ LDL particles (N_{p-1}), and two sink terms: one due to the binding of LDL particles, and another due to

[1] In practice this production term is due to the extraction of intercellular vesicles *i.e.* their recycling [3]. For simplicity, we do not consider how changes in vesicle density influence the production of empty pits. Instead we assume that empty pits are produced at a constant rate $\overline{k}_0$.

internalisation at a rate $\overline{b}$. Combining these mechanisms we have

$$\begin{aligned}
\frac{\mathrm{d}\overline{N}_0}{\mathrm{d}\overline{t}} &= \overline{k}_0 - \overline{a}\overline{L}_e\overline{N}_0 - \overline{b}_0\overline{N}_0, && (3)\\
\frac{\mathrm{d}\overline{N}_p}{\mathrm{d}\overline{t}} &= \overline{a}\overline{L}_e\overline{N}_{p-1} - \overline{b}\,\overline{N}_p - \overline{a}\overline{L}_e\overline{N}_p, \quad (1 \le p \le p_m - 1), && (4)\\
\frac{\mathrm{d}\overline{N}_{p_m}}{\mathrm{d}\overline{t}} &= \overline{a}\overline{L}_e\overline{N}_{p_m-1} - \overline{b}\overline{N}_{p_m}. && (5)
\end{aligned}$$

where $\overline{k}_0$ is the rate at which empty pits are created, $\overline{b}$ is the internalisation rate of pits, and $\overline{b}_0 < \overline{b}$ is the rate at which empty pits are internalised.

The concentration of LDL particles then follows the equations

$$\begin{aligned}
\frac{\mathrm{d}\overline{L}_e}{\mathrm{d}\overline{t}} &= -\overline{a}\overline{L}_e\sum_{p=0}^{p_m-1}\overline{N}_p, \qquad \frac{\mathrm{d}\overline{L}_b}{\mathrm{d}\overline{t}} = \overline{a}\overline{L}_e\sum_{p=0}^{p_m-1}\overline{N}_p - \overline{b}\,\overline{L}_b,\\
\frac{\mathrm{d}\overline{L}_i}{\mathrm{d}\overline{t}} &= \overline{b}\,\overline{L}_b - \overline{k}_{id}\overline{L}_i, \qquad \frac{\mathrm{d}\overline{C}}{\mathrm{d}\overline{t}} = \overline{r}\overline{k}_{id}\overline{L}_i - \overline{\lambda}\,\overline{C},
\end{aligned} \qquad (6)$$

Note that the number of bound LDL particles is given by $\overline{L}_b = \sum_{p=1}^{p_m} p\overline{N}_p(t)$.

The initial conditions for the system of equations (3)–(6) is

$$\begin{gathered}
\overline{N}_0(0) = \overline{n}_0, \quad \overline{L}_e(0) = \overline{L}_0, \quad \overline{L}_b(0) = 0, \quad \overline{L}_i(0) = 0, \quad \overline{C}(0) = 0, \qquad (7)\\
\overline{N}_p(0) = 0, \quad (1 \le p \le p_m)
\end{gathered}$$

that is, the cells have been starved of cholesterol and lipoproteins such that there are no bound or internalised LDL particles, LDLR is maximally expressed, all pits are empty, and there are $\overline{n}_0$ pits with no bound LDL. There is an external source of LDL particles and the cholesterol concentration is zero (alternatively, the concentration variable can be thought of as an excess over the baseline concentration of cholesterol over the level in the starved cell).

2.2 Simplification of model

We introduce the new variable $\overline{S}(t) = \sum_{n=1}^{p_m}\overline{N}_p$ which is the total number of occupied pits on the cell's surface. Combining equations (3)–(5) we have

$$\frac{\mathrm{d}\overline{S}}{\mathrm{d}\overline{t}} = \overline{a}\overline{N}_0\overline{L}_e - \overline{b}\,\overline{S}, \qquad (8)$$

and the equation for $\overline{L}_e$ can be written as

$$\frac{\mathrm{d}\overline{L}_e}{\mathrm{d}\overline{t}} = -\overline{a}\overline{L}_e(\overline{S} + \overline{N}_0 - \overline{N}_{p_m}). \qquad (9)$$

We make the approximation that $\overline{N}_{p_m} \ll \overline{S}$ to obtain the following (closed) system of equations:

$$\begin{aligned}
\frac{\mathrm{d}\overline{L}_e}{\mathrm{d}\overline{t}} &= -\overline{a}\overline{L}_e\overline{N}_0 - \overline{a}\overline{L}_e\overline{S}, \qquad \frac{\mathrm{d}\overline{L}_b}{\mathrm{d}\overline{t}} = \overline{a}\overline{L}_e\overline{N}_0 + \overline{a}\overline{L}_e\overline{S} - \overline{b}\,\overline{L}_b,\\
\frac{\mathrm{d}\overline{L}_i}{\mathrm{d}\overline{t}} &= \overline{b}\,\overline{L}_b - \overline{g}\overline{k}_{id}\overline{L}_i, \qquad \frac{\mathrm{d}\overline{C}}{\mathrm{d}\overline{t}} = \overline{r}\overline{k}_{id}\overline{L}_i - \overline{\lambda}\,\overline{C},\\
\frac{\mathrm{d}\overline{S}}{\mathrm{d}\overline{t}} &= \overline{a}\overline{L}_e\overline{N}_0 - \overline{b}\,\overline{S}, \qquad \frac{\mathrm{d}\overline{N}_0}{\mathrm{d}\overline{t}} = \overline{k}_0 - \overline{a}\overline{L}_e\overline{N}_0 - \overline{b}_0\overline{N}_0.
\end{aligned} \qquad (10)$$

2.3 Re-scaling and parameter values

Our model formulation requires knowledge of the initial concentration of pits (in number per volume) and the initial concentration of extracellular LDL particles (in number per volume). We must also specify the rates at which LDL particles bind, are internalised and produce cholesterol. In Table 2 we list the dimensional values available from the literature. In deriving the model, we have implicitly assumed that concentration variables are measured in number of particles per volume. Thus we need to convert all the concentrations from mass per unit volume to numbers per unit volume.

$\overline{L}_0$: To convert $\overline{L}_0$ from mass per unit volume (as quoted in Table 2) to a number-based concentration we assume that LDL particles are spherical and have the same density as water, (*i.e.* 10^3 kgm^{-3}). Taking the radius of an LDL particle to be 10nm, its volume is $4\pi/3R^3 \approx 4 \times 10^{-24}$ m^3, and its mass is 4×10^{-12} μg. Each μg thus contains 2.5×10^{11} particles, so the concentration $\overline{L}_0$ ranges between (5×10^{11}) and (5×10^{12}) particles per ml.

$\overline{n}_0$: The number $\overline{n}_0$ of empty pits at the start of the experiment can be estimated from the fact that each cell has 80 pits (Table 1) and there are 10^6 cells in the 1ml sample; thus $\overline{n}_0 = 8 \times 10^7$ pits per ml.

Parameter	Description	Estimated value
$\overline{a}$	Rate of LDL binding to pits.	unknown
$\overline{b}$	Rate of internalisation of non-empty pits	log 2/22 s^{-1}
$\overline{b}_0$	Rate of internalisation of empty pits	log 2/50 s^{-1}
$\overline{k}_0$	Rate of formation of new (empty) pits	unknown
$\overline{k}_{id}$	Rate of LDL conversion to cholesterol	1/180 s^{-1}
$\overline{\lambda}$	Rate of cholesterol loss	1/780 s^{-1}
$\overline{L}_0$	Initial concentration of extracellular LDL particles.	2–20μg/ml
$\overline{n}_0$	Initial concentration of pits (all pits empty at $\overline{t} = 0$)	(50–) 80 per cell

Table 2: Dimensional parameters and their values

Parameter	Description	Value
$\overline{L}_0$	Initial concentration of LDL particles.	2.5×10^{12} particles/ml
$\overline{n}_0$	Initial concentration of pits (all empty at $\overline{t} = 0$).	8×10^7 pits/ml

Table 3: Rescaled dimensional parameter values.

b and b_0: In Table 2 the internalisation rate for non-empty and empty pits is given respectively as $\ln(2)/22 \simeq 0.0315$ per sec and $\ln(2)/50 \simeq 0.0139$. Each pit has approximately 250 receptors and therefore this corresponds to the internalisation of 7.88 receptors per sec; since an LDL particle covers approximately 31 receptors (see Table 1), LDL particles are internalised at a rate of 0.254 per sec to non-empty pits and 0.112 per sec in empty pits. These are the appropriate values for b and b_0 respectively.

k_{id} and k: This is the rate at which the internalised LDL particles are converted to internal cholesterol (k_{id}) and the rate at which receptors are recycled to the surface of the cell

(k). The digestion of LDL to cholesterol is a known rate given by $k_{id} = 1/180$ per sec in Table 2. In the absence of any further data we assume that following LDL digestion the associated receptors return to the surface also at the same rate, $k = 1/180$ per sec.

2.4 Non-dimensionalisation

We non-dimensionalise equations (10) as follows:

$$t = \frac{\overline{t}}{\overline{t}_0} \qquad N_0 = \frac{\overline{N}_0}{\overline{n}_0} \qquad S = \frac{\overline{S}}{\overline{n}_0} L_e = \frac{\overline{L}_e}{\overline{L}_0} \qquad L_b = \frac{\overline{L}_b}{\overline{L}_0} \qquad L_i = \frac{\overline{L}_i}{\overline{L}_0} \qquad C = \frac{\overline{C}}{\overline{C}_0}, \tag{11}$$

where overbars denote dimensional quantities.

We choose $\overline{t}_0 = \overline{n}_0/\overline{k}_0$ so that the rate of creation of empty pits is unity in the non-dimensional equations. We also specify $\overline{k}_0 = \overline{n}_0\overline{b}_0$ so that the steady-state of the system is $L_e = L_b = L_i = C = 0$, $N_0 = 1 = S$; this means that in the experimental system, the cells are in a steady state before the LDL is added. The quantity $\overline{C}_0$ is chosen by $\overline{C}_0 = \overline{k}_{id}\overline{L}_0\overline{n}_0/\overline{k}_0$, so that the rate of production from L_i is unity.

Parameter	Description	Value
α	Binding rate of LDL to pits	56
b	Rate of internalisation of pits containing LDL	2.2662
p	ratio of LDL particles to pits at $t = 0$	1.25×10^4
k_{id}	Rate of conversion of LDL to cholesterol	0.40
λ	Rate of loss of internal cholesterol	0.09

Table 4: Non-dimensional parameter values.

The non-dimensional parameter groupings are given by

$$\alpha = \frac{\overline{a}\overline{n}_0^2}{\overline{k}_0}, \qquad b = \frac{\overline{b}\overline{n}_0}{\overline{k}_0}, \qquad p = \frac{1}{q} = \frac{\overline{L}_0}{\overline{n}_0}, \qquad k_{id} = \frac{\overline{k}_{id}\overline{n}_0}{\overline{k}_0}, \qquad \lambda = \frac{\overline{\lambda}\overline{n}_0}{\overline{k}_0}, \tag{12}$$

where we note that $b > 1$ since occupied pits are internalised at a faster rate than empty pits.

We obtain the following non-dimensional model

$$\frac{\mathrm{d}N_0}{\mathrm{d}t} = 1 - \alpha p L_e N_0 - N_0, \tag{13}$$

$$\frac{\mathrm{d}S}{\mathrm{d}t} = \alpha p L_e N_0 - bS, \tag{14}$$

$$\frac{\mathrm{d}L_e}{\mathrm{d}t} = k_L - \alpha L_e S, \tag{15}$$

$$\frac{\mathrm{d}L_b}{\mathrm{d}t} = \alpha L_e S - bL_b \tag{16}$$

$$\frac{\mathrm{d}L_i}{\mathrm{d}t} = bL_b - k_{id}L_i, \tag{17}$$

$$\frac{\mathrm{d}C}{\mathrm{d}t} = L_i - \lambda C, \quad , \tag{18}$$

together with the initial conditions

$$N_0(0) = 1, \qquad S(0) = 1, \qquad L_e(0) = 1, \qquad L_b(0) = 0, \qquad L_i(0) = 0, \qquad C(0) = 0. \tag{19}$$

We note that equations (13)-(15) decouple from the rest of the system.

2.5 Numerical results

Equations (13)–(19) were solved numerically using a Matlab ODE solver (ode45, a medium order Runge-Kutta method for non-stiff problems). Typical solution profiles for external LDL (L_e), bound LDL (L_b), internalised LDL (L_i) and cholesterol (C) are presented in Figure 3. Our results are in good qualitative (and quantitative) agreement with the experimental results presented in Figure 3(b), which are taken from [1]. (Very roughly, our time units correspond to hours.)

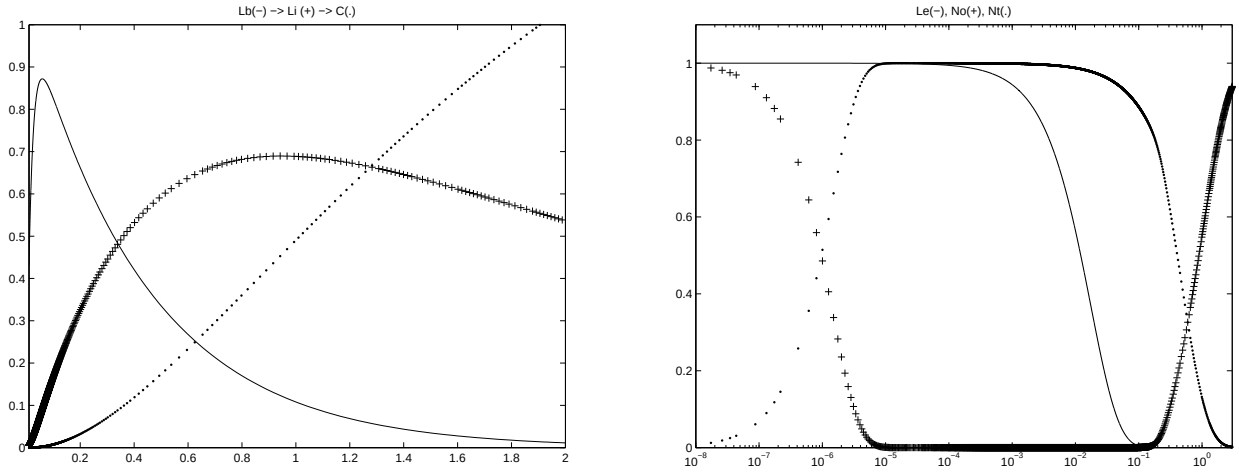

Figure 3: Numerical solution of (13)–(19). (a) The concentrations of bound LDL particles (L_b, solid curve), internalised LDL particles (L_i, denoted with '+' signs) and internal cholesterol level (C, denoted by dots). (b) the concentration of external LDL particles (L_e, solid line), empty pits (N_0, '+'s) and occupied pits (S, dotted line).

The variables N_0, S and L_e drive the system, yet are not measured in the experimental results of Brown & Goldstein [1]. Our predicted evolution of these quantities is displayed in Figure 3(b). Over a very rapid timescale (10^{-6} hours = milliseconds) all the pits become occupied by LDL, we see N_0 decrease from 1 to zero and S increases from zero to 1. However, it takes much longer for the external LDL concentration to decay; this occurs over a timescale of 1-10 minutes. The experimentally measurable quantities of bound LDL increases relatively rapidly over the 1-10 minute timescale and over the longer timescale of an hour the internalised LDL concentration rises to a maximum and starts to decline as the cholesterol content of the cells rises.

It is worth commenting that the system has not reached a steady-state or equilibrium solution by $t = 2$. The variables L_e, S and N_0 are almost at their steady-state values of zero, zero and unity respectively. Whilst L_b is clearly close and approaching its steady value of zero, the observables L_i and C, at $t = 2$, L_i has only just peaked and is starting a long slow decline to zero and C is still increasing, has yet to reach a maximum before also approaching zero.

We have studied the effects of doubling and halving each of the parameters a, b, k_{id} and λ. There is little qualitative change in the results, which suggests that the model is robust. The model appears most sensitive to the rate of pit internalisation, b, as shown in Figure 5, where the numerical simulations reported in Figure 3 are reevaluated with values of b twice and one half of the original value. Increasing b (so that the pits were internalised more rapidly) increased the peak value of internalised LDL and also led to an increase in the intracellular cholesterol content.

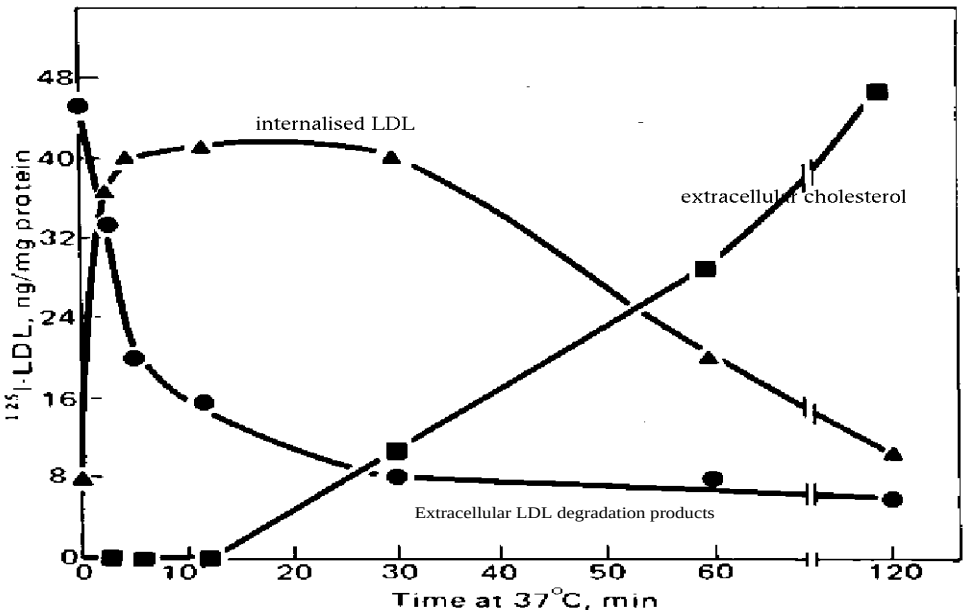

Figure 4: Data from [1], for comparison with Figure 3(a). Bound LDL corresponds to our L_b, internalised LDL to our L_i and degraded to our C.

2.6 Asymptotic solution

We focus on just (13)–(15), in which $p \gg 1$ is a large parameter, and are subject to the initial conditions $N_0(0) = 1$, $S(0) = 0$ and $L_e(0) = 1$.

2.6.1 Region 1: rapid adjustment from ICs

Define $\tau_1 = pt$ then

$$\frac{\mathrm{d}N_0}{\mathrm{d}\tau_1} = \frac{1}{p} - \alpha L_e N_0 - \frac{N_0}{p}, \qquad \frac{\mathrm{d}S}{\mathrm{d}\tau_1} = \alpha L_e N_0 - \frac{bS}{p}, \qquad \frac{\mathrm{d}L_e}{\mathrm{d}\tau_1} = -\frac{\alpha L_e (N_0 + S)}{p}. \tag{20}$$

Thus over this timescale L_e remains constant whilst N_0 decreases and S increases according to

$$L_e = 1, \qquad N_0 = \mathrm{e}^{-\alpha\tau_1}, \qquad S = 1 - \mathrm{e}^{-\alpha\tau_1}. \tag{21}$$

This solution ceases to be valid when $\alpha N_0 L_e \sim 1/p$, that is, when $\tau_1 = (1/\alpha)\log p$; at this time $S = 1$ and $L_e = 1$.

2.6.2 Region 2: the first slow phase

In this region, N_0 is small, having reached $\mathcal{O}(1/p)$ in the first region. Thus we put $N_0 = (1/p)N_1(t)$, and so obtain

$$\frac{1}{p}\frac{\mathrm{d}N_1}{\mathrm{d}t} = 1 - \alpha L_e N_1 - \frac{N_1}{p}, \qquad \frac{\mathrm{d}S}{\mathrm{d}t} = \alpha L_e N_1 - bS, \qquad \frac{\mathrm{d}L_e}{\mathrm{d}t} = -\alpha L_e \left(\frac{N_1}{p} + S\right). \tag{22}$$

From the first equation we have $N_1 = 1/\alpha L_e$ throughout this region, hence the solution of the second and third equations can also easily be derived

$$S = \frac{1}{b}\left(1 + (b-1)\mathrm{e}^{-bt}\right), \quad L_e = \exp\left(-\frac{\alpha}{b^2}\left[bt + (b-1)(1-\mathrm{e}^{-bt})\right]\right), \quad N_0 = \frac{1}{p\alpha L_e}. \tag{23}$$

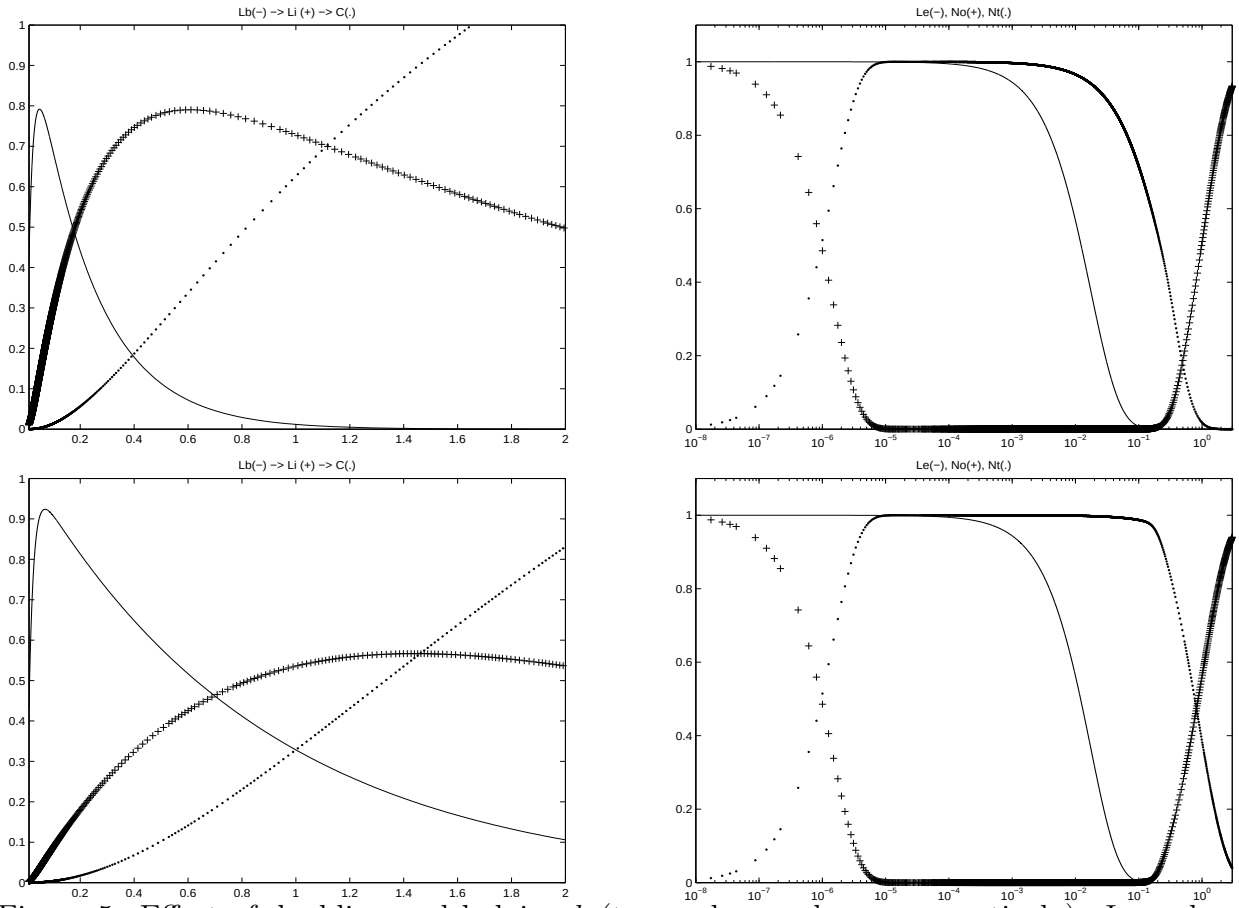

Figure 5: Effect of doubling and halving b (top and second row, respectively). In each case: (left) the concentrations of bound LDL (L_b, solid curve), internalised LDL (L_i, '+' signs) and internal cholesterol (C, dots); (right) the concentrations of external LDL (L_e, solid line), empty pits (N_0, '+'s) and occupied pits (S, dotted line).

This solution cannot hold indefinitely: eventually the exhaustion of L_e ($L_e \to 0$ as $t \to \infty$) will mean that $\alpha p L_e N_0$ cannot be sustained, and N_0 will rise above $\mathcal{O}(1/p)$ over a longer timescale. This timescale ends when $N_0 = \mathcal{O}(1)$ and $L_e = \mathcal{O}(1/p)$, which is when $t = t_c := (b/\alpha)\log(p) + 1/b - 1$. At $t = t_c$, $N_0 = 1/\alpha$ and $S = 1/b$.

2.6.3 Region 3: the second slow phase

In this phase of the process, L_e is small, we write it as $L_e = (1/p)L_1$ whilst N_0 and S are both $\mathcal{O}(1)$. The timescale is still $\mathcal{O}(1)$, but shifted by an amount t_c. The governing equations are thus

$$\frac{\mathrm{d}N_0}{\mathrm{d}t} = 1 - \alpha L_1 N_0 - N_0, \qquad \frac{\mathrm{d}S}{\mathrm{d}t} = \alpha N_0 L_1 - bS, \qquad \frac{\mathrm{d}L_1}{\mathrm{d}t} = -\alpha L_1(N_0 + S). \tag{24}$$

Since no terms are ignored in this regime, we cannot find an explicit solution. However, at larger times the solution can be approximated by combinations of exponentials. Matching the

arbitrary constants to the behaviour at the end of region 2, we obtain

$$\begin{aligned} N_0 &\sim 1 - \frac{(2\alpha - 1 - 2\alpha^2)}{\alpha(1-\alpha)} p^{b/\alpha} \mathrm{e}^{1/b - 1 - t} - \frac{\alpha}{(1-\alpha)} p^b \mathrm{e}^{\alpha/b - \alpha - \alpha t}, \\ S &\sim \frac{(b - \alpha - \alpha b)}{b(b-\alpha)} p^{b^2/\alpha} \mathrm{e}^{1 - b - bt} + \frac{\alpha}{(b-\alpha)} p^b \mathrm{e}^{\alpha/b - \alpha - \alpha t}, \\ L_e &\sim p^{b-1} \mathrm{e}^{\alpha/b - \alpha - \alpha t}. \end{aligned} \tag{25}$$

It is hoped that in future work, such an approach will yield simple explicit approximations for the evolution of the observed quantities L_b, L_i, C.

2.7 Summary

In this section we have outlined a model of LDL uptake by cells in which the geometric constraints of receptors being located in pits is taken into account. The results of the model agree well with the experimental data of Brown & Goldstein [1]. However, the model does not include the effects of VLDL competing with LDL for receptors on the surface of the cell.

3 Modelling LDL and VLDL uptake by the liver

In this section we formulate a model to consider the effects that combinations of LDL, VLDL-2 and VLDL-3 binding and internalisation have on the total cholesterol content of the liver.

The internalisation of LDL and VLDL particles along with the respective receptors involved on the surface of the liver is governed by the following reactions. In the case of LDL binding to the liver surface, the reaction sequence is as follows:

$$MR_F + L_e \xrightarrow{\alpha_L} L_B \xrightarrow{\beta_L} MR_I + L_I \xrightarrow{\gamma_L} MR_F + R_L^{\mathrm{chol}} C. \tag{26}$$

Here M represents the number of free receptors R_F which are covered when a free LDL particle L_e binds to the lipoprotein pits on the cell surface at a rate α_L. Here R_F refers to the total density of free receptors on the surface of the liver. The bound LDL particle L_B and bound receptors are then ingested by the cell to become internalised LDL L_I and receptors R_I respectively, at a rate β_L. The ingested receptors are then returned to the cell surface at a rate γ_L in the form of new pits whilst the ingested LDL is converted to R_L^{chol} molecules of cholesterol, denoted C.

The binding and internalisation of VLDL-2 and VLDL-3 follow similar reactions

$$NR_F + V_{E2} \underset{\alpha_-}{\overset{\alpha_2}{\rightleftharpoons}} V_{B2} \xrightarrow{\beta_v} NR_I + (h_2 - 1)V_{I2} \xrightarrow{\gamma_v} NR_F + (h_2 - 1)R_{V2}^{\mathrm{chol}} C \tag{27}$$

$$QR_F + V_{E3} \underset{\alpha_-}{\overset{\alpha_3}{\rightleftharpoons}} V_{B3} \xrightarrow{\beta_v} QR_I + (h_3 - 1)V_{I3} \xrightarrow{\gamma_v} QR_F + (h_3 - 1)R_{V3}^{\mathrm{chol}} C. \tag{28}$$

where N and Q are the number of free receptors covered by the binding of VLDL-2 and VLDL-3 particles to the liver surface respectively and V_{Ei}, V_{Bi} and V_{Ii} $(i = 2, 3)$ are the extracellular, bound and internalised VLDL (of types two and three). We note that our formulation accounts for receptors which are bound by the respective LDL and VLDL particles as well as those which are covered by the particles due to the binding process.

In general, i.e. if $N \neq Q$, then the rates of VLDL binding, α_2 and α_3, will have different units. The inclusion of the parameters h_2 and h_3 allows us to assess the effect of internalisation ($h_2 = h_3 = 2$) or no internalisation ($h_2 = h_3 = 1$) of VLDL-2 or VLDL-3; or the internalisation of one but not the other ($h_2 = 2$ with $h_3 = 1$). We note that the effects of VLDL unbinding from the surface can also be considered, and the rate of this reaction can be considered to be the same for both VLDL-2 and VLDL-3, namely α_-.

Applying the law of mass action to reactions (26)-(28) yields the following ordinary differential equations; LDL binding is governed by

$$\begin{aligned}
\frac{\mathrm{d}l_E}{\mathrm{d}t} &= -\alpha_L \rho_F^M l_E && (29)\\
\frac{\mathrm{d}l_B}{\mathrm{d}t} &= \alpha_L \rho_F^M l_E - \beta_L l_B && (30)\\
\frac{\mathrm{d}l_I}{\mathrm{d}t} &= \beta_L l_B - \gamma_L l_I, && (31)
\end{aligned}$$

where $l_E = [L_e]$, $\rho_F = [R_F]$, $l_B = [L_B]$ and $l_I = [L_I]$. Similar variables are used to represent the respective concentrations of free, bound and internalised VLDL particles in the following equations,

$$\begin{aligned}
\frac{\mathrm{d}v_{E2}}{\mathrm{d}t} &= -\alpha_2 \rho_F^N v_{E2} + \alpha_- v_{B2}, && (32)\\
\frac{\mathrm{d}v_{B2}}{\mathrm{d}t} &= \alpha_2 \rho_F^N v_{E2} - \alpha_- v_{B2} - \beta_v (h_2 - 1) v_{B2}, && (33)\\
\frac{\mathrm{d}v_{I2}}{\mathrm{d}t} &= \beta_v (h_2 - 1) v_{B2} - \gamma_v (h_2 - 1) v_{I2}, && (34)
\end{aligned}$$

and

$$\begin{aligned}
\frac{\mathrm{d}v_{E3}}{\mathrm{d}t} &= -\alpha_3 \rho_F^Q v_{E3} + \alpha_- v_{B3}, && (35)\\
\frac{\mathrm{d}v_{B3}}{\mathrm{d}t} &= \alpha_3 \rho_F^Q v_{E3} - \alpha_- v_{B3} - \beta_v (h_3 - 1) v_{B3}, && (36)\\
\frac{\mathrm{d}v_{I3}}{\mathrm{d}t} &= \beta_v (h_3 - 1) v_{B3} - \gamma_v (h_3 - 1) v_{I3}, && (37)
\end{aligned}$$

respectively.

The change in free receptor density is governed by

$$\begin{aligned}
\frac{\mathrm{d}\rho_F}{\mathrm{d}t} = -\alpha_L M l_e \rho_F^M - \alpha_2 N v_{E2} \rho_F^N - \alpha_3 Q v_{E3} \rho_F^Q + \alpha_- N v_{B2} + \alpha_- Q v_{B3} \\
+ \gamma_L M l_I + \gamma_v N (h_2 - 1) v_{I2} + \gamma_v Q (h_3 - 1) v_{I3}.
\end{aligned} \qquad (38)$$

We note the total bound and internalised receptor densities are given by

$$\rho_B = M l_B + N v_{B2} + Q v_{B3} \quad \text{and} \quad \rho_I = M l_I + N v_{I2} + Q v_{I3},$$

respectively and the total receptor density

$$\rho_T = \rho_F + \rho_B + \rho_I, \qquad (39)$$

is conserved. The cholesterol ingested by the liver is given by

$$\frac{\mathrm{d}C}{\mathrm{d}t} = \gamma_L R_L^{chol} L_I + \gamma_v R_{V-2}^{chol} V_{I2} + \gamma_v R_{V-3}^{chol} V_{I3}, \tag{40}$$

where R_L^{chol} , R_{V2}^{chol} and R_{V3}^{chol} represent the quantity of cholesterol per LDL, VLDL-2 and VLDL-3 particle respectively.

The initial conditions for the above equations are defined by

$$\begin{gathered} l_E(0) = l_0, \qquad l_B(0) = 0, \qquad l_I(0) = 0, \qquad v_{E2}(0) = v_{02}, \qquad v_{B2}(0) = 0, \\ v_{I2}(0) = 0, \qquad v_{E3}(0) = v_{03}, \qquad v_{B3}(0) = 0, \qquad v_{I3}(0) = 0, \\ \rho_F = \rho_0 \quad \text{and} \quad C(0) = 0. \end{gathered} \tag{41}$$

3.1 Non-dimensionalisation

The governing equations are non-dimensionalised according to the following re-scalings

$$\begin{gathered} t = \frac{\widehat{t}}{\alpha_L M \rho_0^M}, \qquad l_E = l_0 \widehat{l}_E, \qquad l_B = l_0 \widehat{l}_B, \qquad l_I = l_0 \widehat{l}_I, \\ v_{E2} = v_{02}\widehat{v}_{E2}, \qquad v_{B2} = v_{02}\widehat{v}_{B2}, \qquad v_{I2} = v_{02}\widehat{v}_{I2}, \\ v_{E3} = v_{02}\widehat{v}_{E3}, \qquad v_{B3} = v_{02}\widehat{v}_{B3}, \qquad v_{I3} = v_{02}\widehat{v}_{I3}, \\ \rho_F = \rho_0 \widehat{u}^{1/M} \quad \text{and} \quad C = C_0 \widehat{c}. \end{gathered} \tag{42}$$

The nonlinear substitution included in the non-dimensionalisation of ρ_F is to allow stable numerical solutions of the resulting system to be derived (raising the variable ρ_F to large powers such as M, N, Q can result in numerical inaccuracies). We will ignore the terms such as $\widehat{u}^{1/M}$ in the resulting equations, since $\widehat{u} = \mathcal{O}(1)$ and $M \gg 1$. Care needs to be exercised with the manipulation of terms involving α_L and $\alpha_{2,3}$ since these parameters have quite strange units.

$$\frac{\mathrm{d}\widehat{l}_E}{\mathrm{d}\widehat{t}} = -\frac{\widehat{l}_E \widehat{u}}{M}, \tag{43}$$

$$\frac{\mathrm{d}\widehat{l}_B}{\mathrm{d}\widehat{t}} = \frac{\widehat{u}\widehat{l}_E}{M} - \beta \widehat{l}_B, \tag{44}$$

$$\frac{\mathrm{d}\widehat{l}_I}{\mathrm{d}\widehat{t}} = \beta \widehat{l}_B - \gamma \widehat{l}_I, \tag{45}$$

$$\frac{\mathrm{d}\widehat{v}_{E2}}{\mathrm{d}\widehat{t}} = \psi \widehat{v}_{B2} - \phi_2 \widehat{u}^n \widehat{v}_{E2}, \tag{46}$$

$$\frac{\mathrm{d}\widehat{v}_{B2}}{\mathrm{d}\widehat{t}} = \phi_2 \widehat{u}^n \widehat{v}_{E2} - \psi \widehat{v}_{B2} - \chi(h_2 - 1)\widehat{v}_{B2}, \tag{47}$$

$$
\begin{aligned}
\frac{\mathrm{d}\widehat{v}_{I2}}{\mathrm{d}\widehat{t}} &= (h_2-1)(\chi\widehat{v}_{B2}-\omega\widehat{v}_{I2}), && (48)\\
\frac{\mathrm{d}\widehat{v}_{E3}}{\mathrm{d}\widehat{t}} &= \psi\widehat{v}_{B3}-\phi_3\widehat{u}^q\widehat{v}_{E3}, && (49)\\
\frac{\mathrm{d}\widehat{v}_{B3}}{\mathrm{d}\widehat{t}} &= \phi_3\widehat{u}^q\widehat{v}_{E3}-\psi\widehat{v}_{B3}-\chi(h_3-1)\widehat{v}_{B3}, && (50)\\
\frac{\mathrm{d}\widehat{v}_{I3}}{\mathrm{d}\widehat{t}} &= (h_3-1)(\chi\widehat{v}_{B3}-\omega\widehat{v}_{I3}), && (51)\\
\sigma\frac{\mathrm{d}\widehat{u}}{\mathrm{d}\widehat{t}} &= \gamma\widehat{l}_I\widehat{u}-\frac{\widehat{l}_E\widehat{u}^2}{M}+nr\widehat{u}\left[(h_2-1)\omega\widehat{v}_{I2}+\psi\widehat{v}_{B2}-\phi_2\widehat{u}^n\widehat{v}_{E2}\right]+\\
&\quad +qr\widehat{u}\left[(h_3-1)\omega\widehat{v}_{I3}+\psi\widehat{v}_{B3}-\phi_3\widehat{u}^q\widehat{v}_{E3}\right], && (52)\\
\frac{\mathrm{d}\widehat{c}}{\mathrm{d}\widehat{t}} &= \lambda\left(\gamma R_L^{\mathrm{chol}}\widehat{l}_I+\omega rR_{V2}^{\mathrm{chol}}\widehat{v}_{I2}+\omega rR_{V3}^{\mathrm{chol}}\widehat{v}_{I3}\right), && (53)
\end{aligned}
$$

where

$$
\begin{gathered}
n=\frac{N}{M},\qquad q=\frac{Q}{M},\qquad r=\frac{v_{02}}{l_0},\qquad \lambda=\frac{l_0}{C_0},\qquad \beta=\frac{\beta_L}{M\alpha_L\rho_0^M},\qquad \gamma=\frac{\gamma_L}{M\alpha_L\rho_0^M},\\
\phi_2=\frac{\alpha_2\rho_0^{N-M}}{M\alpha_L},\qquad \phi_3=\frac{\alpha_3\rho_0^{Q-M}}{M\alpha_L},\qquad \psi=\frac{\alpha_-}{M\alpha_L\rho_0^M},\qquad \chi=\frac{\beta_v}{M\alpha_L\rho_0^M},\qquad (54)\\
\omega=\frac{\gamma_v}{M\alpha_L\rho_0^M}\quad\text{and}\quad \sigma=\frac{\rho_0}{M^2l_0}.
\end{gathered}
$$

The initial conditions for the non-dimensional system of equations are

$$
\begin{gathered}
\widehat{l}_E(0)=1,\qquad \widehat{l}_B(0)=0,\qquad \widehat{l}_I(0)=0,\qquad \widehat{v}_{E2}(0)=1,\qquad \widehat{v}_{B2}(0)=0,\\
\widehat{v}_{I2}(0)=0,\qquad \widehat{v}_{E3}(0)=v_0,\qquad \widehat{v}_{B3}(0)=0,\qquad \widehat{v}_{I3}(0)=0,\qquad (55)\\
\widehat{\rho}_F=\rho_0\quad\text{and}\quad \widehat{c}(0)=0.
\end{gathered}
$$

In the work which follows the hats will be dropped.

3.2 Parameter values

Our model formulation requires knowledge of the initial number of free receptors per liver cell, the average number of receptors covered by LDL and VLDL of types one and two and the respective rates of binding, internalisation and rate of return of receptors to the liver surface.

Many of the parameters can be found from the earlier model (see Table 2):

β_L: In Table 2 the internalisation rate for pits is given as $\ln(2)/22 \simeq 0.0315$ per sec. This corresponds to the internalisation of 7.88 receptors per sec; since an LDL particle covers M=31 receptors, LDL particles are internalised at a rate of 0.254 per sec – this is an appropriate value for β_L.

β_V: Following the above argument: since VLDL particles cover ∼70 receptors, they are internalised at a rate of 0.113 per second – the value of β_V.

α_L: From the model presented in Section 2, we see that the initial rate of loss of L_e is $(1/L_e)\mathrm{d}L_e/\mathrm{d}t = -aS_0$. Since $S_0 = 50$ and $a = b/L_0\bar{b}$ we have $a = \ln(2)/22 \times 0.8 \times 6 \approx 0.006$, so $aS_0 = 0.33$ per sec. In our model, the initial dimensional rate of loss of external LDL is $(1/l_E)\mathrm{d}l_E/\mathrm{d}t = -\alpha_L\rho_0^M$, thus we expect $\alpha_L\rho_0^M = 0.33$ per sec as well.

Parameter	Description	Value
M	Total number of free receptors covered by a bound LDL particle	31
N	Total number of free receptors covered by a bound VLDL-2 particle	70
Q	Total number of free receptors covered by a bound VLDL-3 particle	70
α_L	Rate of LDL binding to free receptors	0.0002
β_L	Rate of LDL internalisation	0.254 s^{-1}
γ_L	Rate of receptor recycling with respect to LDL binding	$\sim 1/180$ s^{-1}
α_2	Rate of VLDL-2 binding to free receptors	α_L
α_3	Rate of VLDL-3 binding to free receptors	α_L
α_-	Rate of VLDL unbinding from receptors	0 s^{-1}
β_v	Rate of VLDL-2 and VLDL-3 internalisation	0.112 s^{-1}
γ_v	Rate of receptor recycling with respect to VLDL-2 and VLDL-3 binding	$\sim 1/180$ s^{-1}
R_L^{chol}	Average cholesterol content per LDL particle	3400
R_{V-2}^{chol}	Average cholesterol content per VLDL-2 particle	3100
R_{V-3}^{chol}	Average cholesterol content per VLDL-3 particle	3900
ρ_0	Initial concentration of free receptors	2.45×10^4 receptors/cell
l_0	Initial concentration of LDL particles	10μg/ml
v_{02}	typical concentration of VLDL particles	2.5, 10 and 20μg/ml

Table 5: Dimensional parameter values.

Parameter	Description	Value
l_0	Initial conc of LDL particles	2.5×10^{12} particles/ml
v_{02}	Initial conc of LDL particles	2.5×10^{10}, 10^{11}, 2×10^{11} particles/ml
ρ_0	Initial conc of free receptors	2.45×10^{12} receptors/ml

Table 6: Rescaled dimensional parameter values.

γ_L**:** This is the rate at which the internalised LDL particles are converted to cholesterol and the rate at which receptors are recycled to the surface of the cell. The digestion of LDL to cholesterol is a known rate in Section 2, given by $k_{id} = 1/180$ per sec, so we take the same value for γ_L, and, in the absence of any further data on VLDL, we assume that cholesterol from VLDL particles is digested at the same rate, and all associated receptors return to the surface also at the same rate, $\gamma_v = 1/180$ per sec.

$\alpha_{2,3}$**:** unknown. From the non-dimensionalised model, some values can be deduced by comparison with the attachment rate of LDL particles, which is known from the calibration of the model in Section 2. Since $\alpha_L\rho_0^M \approx 0.33$ per sec, we expect $\alpha_2\rho_0^N$ to be at least this, otherwise it would be impossible for VLDL to have any rôle in blocking LDL-binding.

$\alpha\_$**:** taken to be zero for simplicity, if non-zero, then we still expect the reaction to be forward-dominated.

In deriving the model, we have implicitly assumed that concentration variables are measured in number of particles per volume. Thus we need to convert all the concentrations from mass per unit volume to numbers per unit volume:

$l_0 = 10\mu$**g/ml:** LDL particles have a typical radius of 10nm, therefore each has a volume of 4×10^{-24} m^3, (or 4×10^{-18} ml). Assuming the density of LDL particles is similar to that of water (10^3 kg/m^3), we can find out how many LDL particles occupy 10 μ g. The mass of one LDL particle is thus 4×10^{-21} kg $= 4 \times 10^{-12}\mu$g. Thus 10μg represents 2.5×10^{12} particles.

$v_{02} = 2.5, 10$ **and** 20μ**g/ml:** We follow a similar calculation to that above for LDL. VLDL particles typically have a radius of 30 nm, therefore a volume of 27 times that of an LDL particle. The number in 10 μg is thus $1/27^{\text{th}}$ that of LDL (assuming that the densities are the same), namely 10^{11} VLDL particles. For $v_{02} = 20\mu$g/ml we have twice this value, and for $v_{02} = 2.5\mu$g/ml we have one quarter of it.

$\rho_0 = 2.45 \times 10^4$ **receptors per cell:** This also needs to be converted to numbers of receptors per unit volume, and for this we need to know the number of cells per unit volume. Assume a cell has a length of 10μm and therefore a radius of 5μm, then its volume is 10^{-15} m^3 or 10^{-12} l $= 10^{-9}$ ml. So at maximum packing capacity we would have 10^9 cells per ml, at a 10% volume fraction of cells, we have 10^8 cells per ml. This latter figure gives 2.45×10^{12} receptors per ml.

These rescaled values are summarised in Table 6 and allow us to calculate the non-dimensional values detailed in Table 7.

Parameter	Description	Value
n	Relative size of VLDL-2 to LDL.	2.3
q	Relative size of VLDL-3 to LDL.	2.3
r	Ratio of VLDL conc. to LDL conc.	0.25, 1, 2.
λ	Ratio of initial LDL conc. to initial cholesterol.	1
β	Rate of LDL internalisation.	0.016
γ	Rate of receptor recycling with respect to LDL binding.	1/90
$\phi_{2,3}$	Rate of VLDL-2 / VLDL-3 binding to free receptors.	1
ψ	Rate of VLDL-2 and VLDL-3 unbinding from receptors.	0
χ	Rate of internalisation of bound VLDL particles.	0.007
ω	Rate of digestion of internalised VLDL to cholesterol. –also the rate of recycling of receptors back to the cell surface.	1/90
σ	Ratio of receptor- to LDL-concentrations (rescaled).	0.01

Table 7: Non-dimensional parameter values.

3.3 Numerical results

The system of governing equations (43) - (53), with the respective initial conditions, was solved using the ordinary differential equation solver ode15s in Matlab. Parameter values used are those detailed in Table 7.

Figure 7 shows the change in extracellular, bound and internalised LDL concentrations and the change in free receptor density in time. These results show the decrease in extracellular LDL (Figure 7(a)) as it is absorbed by the hepatocyte. The initial free receptor distribution means some particles bind immediately (explaining the rapid rise in bound LDL), after which there exists competition between bound LDL and those in the surrounding suspension for binding to the surface. Given the rapid rate of internalisation the concentration of bound receptors drops off quickly, with the LDL becoming internalised as shown in Figure 7(c). The smooth transient decrease in bound LDL is a result of a balance between the rates of extracellular binding and internalisation. Eventually all the LDL is internalised and following an initial decrease in receptor density, the receptors, due to recycling, are returned to the cell surface as shown in Figure 7(d).

Introducing VLDL, which blocks free receptors, but is not internalised, did not alter the steady-state value of cholesterol internalised by the cell (results not shown). Instead it merely delayed the time taken for the cholesterol to reach a steady-state value. This result is not surprising given that VLDL particles cover more free receptors than LDL and merely block the ability of the latter to attach and become internalised. However, given enough time, due to receptor recycling from the internalisation of even small quantities of LDL, most of the LDL particles will become internalised so long as the rate of attachment of VLDL particles to the cell surface is of the same order of magnitude or greater than that of LDL particle attachment.

Allowing LDL and VLDL particles to both bind to the cell surface and become internalised leads to slightly more complex dynamics than for LDL-only internalisation. We note from Figures 8(a), that the extracellular LDL concentration decreases more rapidly than that of VLDL-1 and VLDL-2 given the reduced size of LDL particles. The initial rapid increase in bound LDL particles is again due to the initial condition that the cell surface is devoid of any particles which may hinder attachment. However, over time the effect of VLDL binding and that of LDL results in a slow decrease in the amount of bound particles, a result also of the

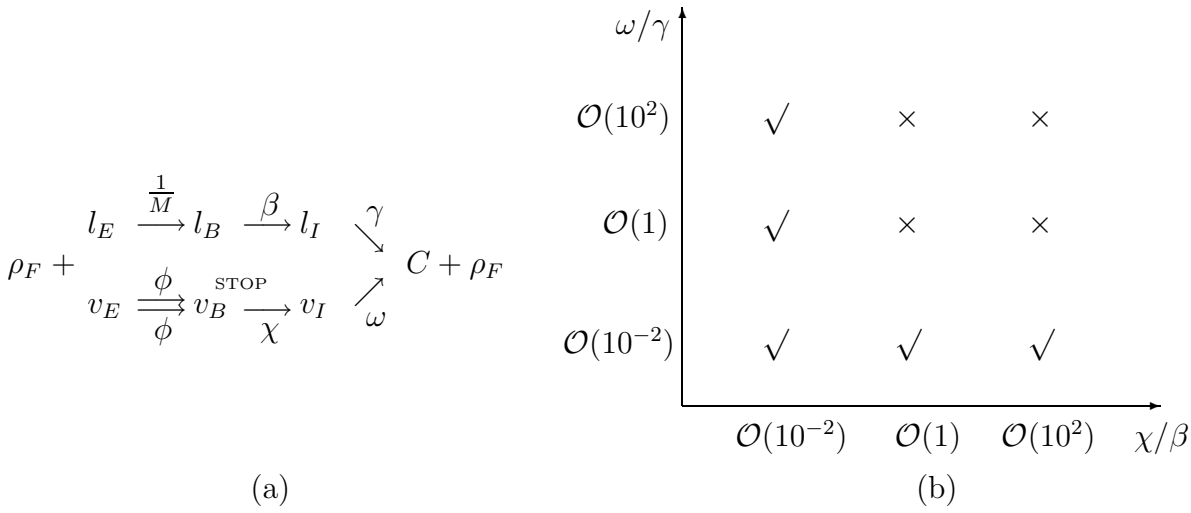

Figure 6: (a) Illustration of the pathways of LDL and VLDL binding and digestion modelled. The top pathway represents unhindered LDL binding ($1/M$), internalisation (at rate β) and digestion (at rate γ). The bottom pathway shows the binding (at rate $\phi_{2,3} > 1/M$), internalisation (rate χ) and digestion (rate ω) of VLDL. The pathway in the centre, which ends at 'STOP' represents the blocking of VLDL with no internalisation. (b) Illustration of the $\chi/\beta - \omega/\gamma$ parameter space, together with an indication of where the experimentally-observed behaviour is expected to occur.

internalisation of each particle as shown in Figures 8(c),(f) and (i).

When both LDL and VLDL particles can both attach and be internalised there are three potential pathways for the conversion of external LDL or VLDL into cholesterol inside the cell (see Figure 6). In order for the VLDL to play a role in inhibiting LDL binding, we have assigned a larger value to the VLDL binding rates $\phi_{2,3}$ than for the LDL binding rate (which is $1/M \approx 0.03$). Thus the journey of VLDL across the lower pathway is quicker than that of LDL across the upper pathway at the start. If this rate faster rate was to continue for the remaining steps (i.e. $\chi \gg \beta$ and $\omega \gg \gamma$) then the cholesterol level would grow faster in the presence of VLDL than for the case of LDL alone. Hence for the rate of cholesterol release to be less when VLDL is present, we need either $\chi \ll \beta$ or $\omega \ll \gamma$ or both.

The change in free receptor density is shown in Figure 9(a). In this case little VLDL (of either type) becomes bound to the cell surface and is subsequentially internalised. The quantity of LDL is greater (again a result of difference in particle size and internalisation rates) than that of VLDL. The concentration of free receptors (for the time period shown) tends towards a steady-state value.

The effect of the LDL only binding, VLDL blockage and internalisation of each particle type is most clearly quantified in a comparison of the quantity of cholesterol internalised by the liver in each case as shown in Figure 9(b). We note firstly that the time-scale over which cholesterol is internalised for the LDL only binding case is considerably more rapid than when VLDL particles are present. This is somewhat expected given VLDL particles cover more surface receptors and hence block the ability of LDL to bind to the liver surface and become internalised. VLDL blockage results in the lowest amount of cholesterol being ingested by the liver, whilst VLDL binding still blocks LDL binding, but due to internalisation of the particles, the total cholesterol content of the liver is somewhat higher.

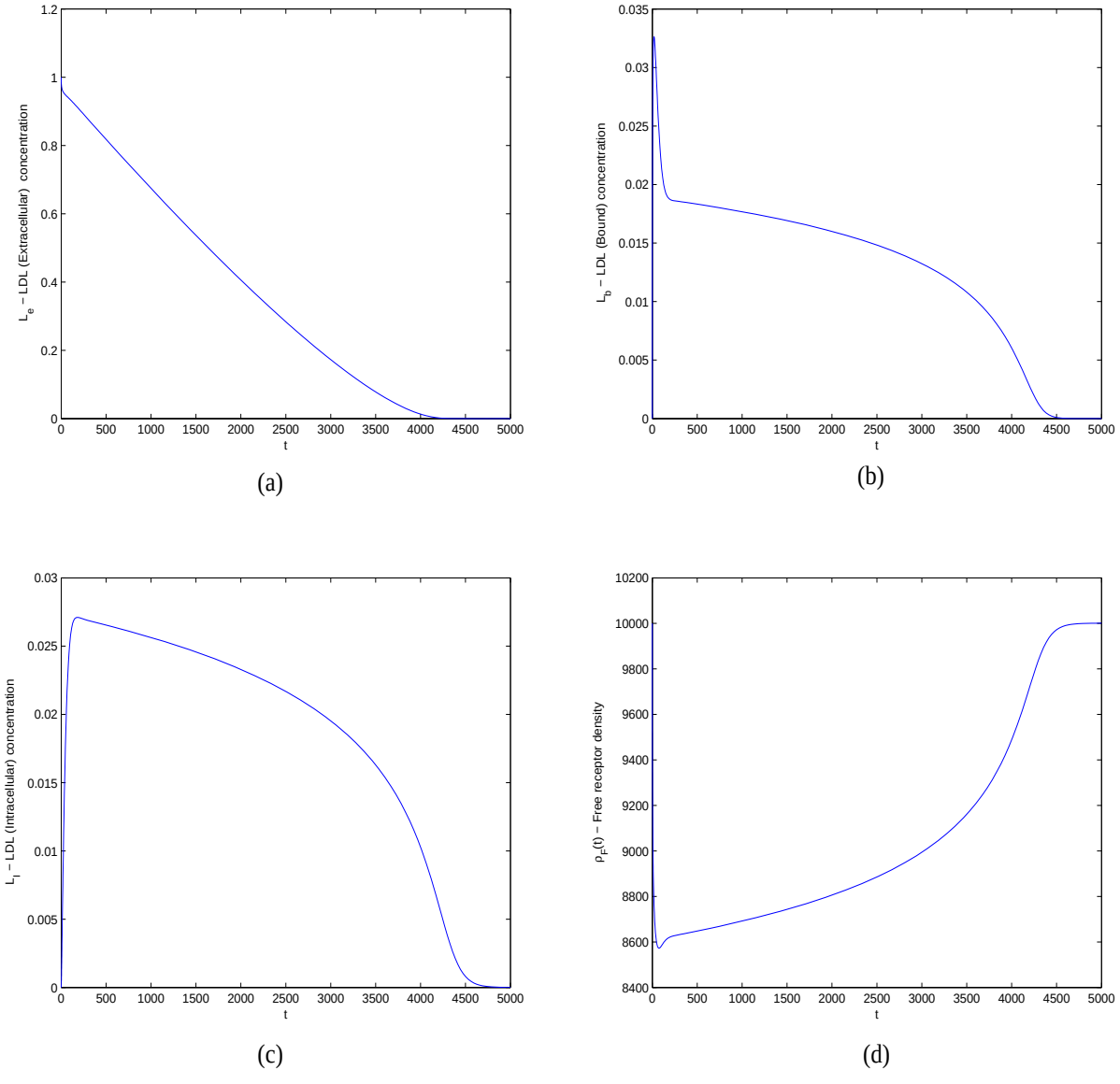

Figure 7: The change in (a) extracellular, (b) bound and (c) internalised LDL and the (d) free receptor density for the case of LDL binding and internalisation. Values are those as detailed in Table 7.

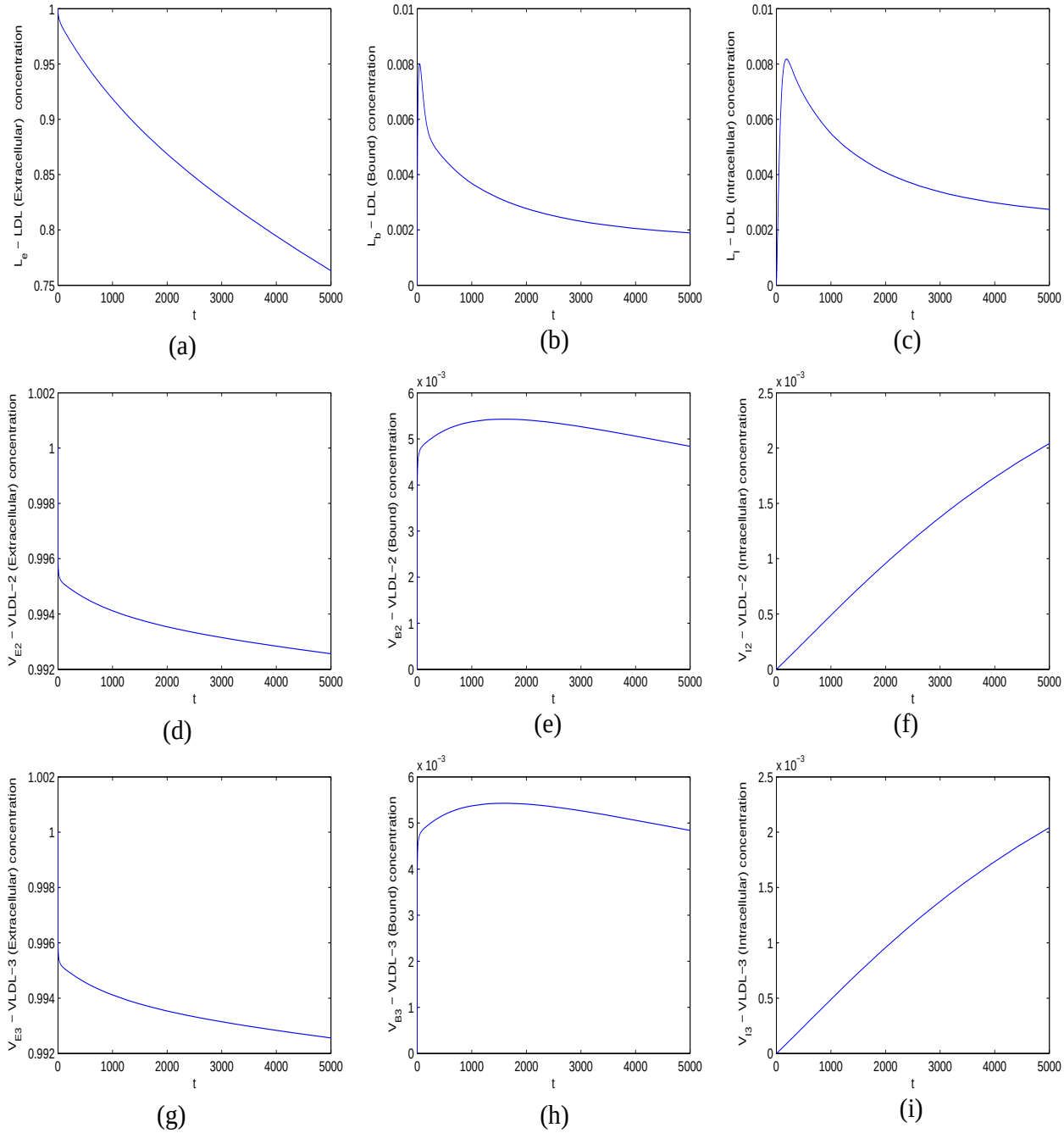

Figure 8: The change in the respective concentrations of (a) extracellular LDL, (b) bound LDL, (c) internalised LDL, (d) extracellular VLDL-2, (e) bound VLDL-2, (f) internalised VLDL-2, (g) extracellular VLDL-3, (e) bound VLDL-3 and (f) internalised VLDL-3 and VLDL. Here $r = 2$, $\chi = 2.5 \times 10^{-3}$ and $\omega = 1$.

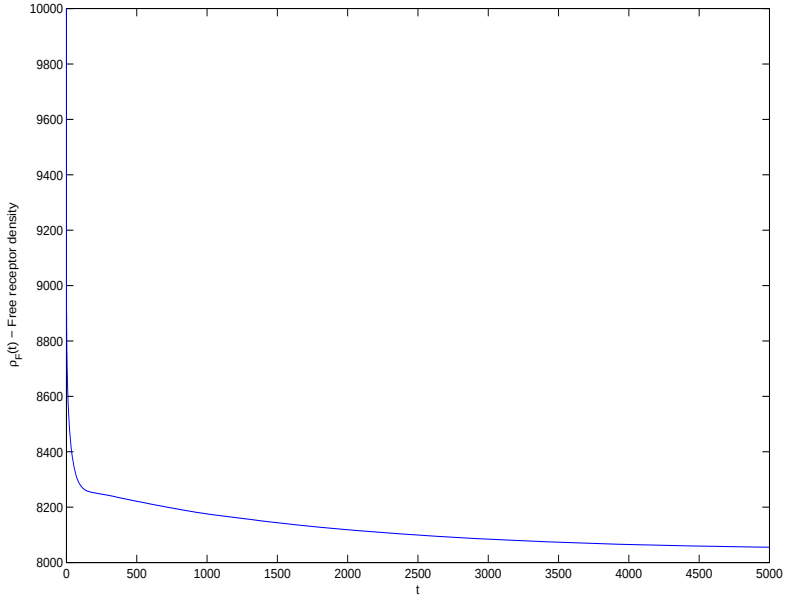

(a)

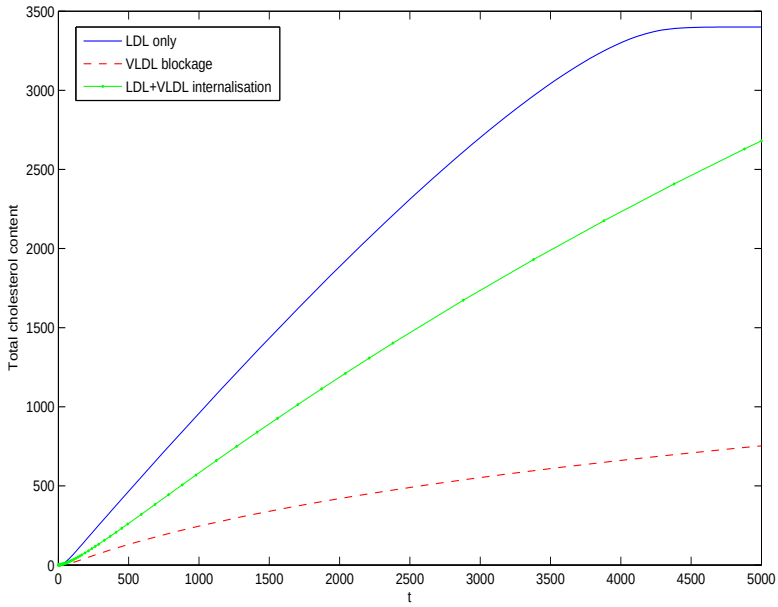

(b)

Figure 9: (a) The change in free receptor density for the case of LDL and VLDL binding and internalisation. (b) The difference in total cholesterol uptake by the liver for each of the three scenarios. In each case $r = 2$, $\chi = 2.5 \times 10^{-3}$ and $\omega = 1$.

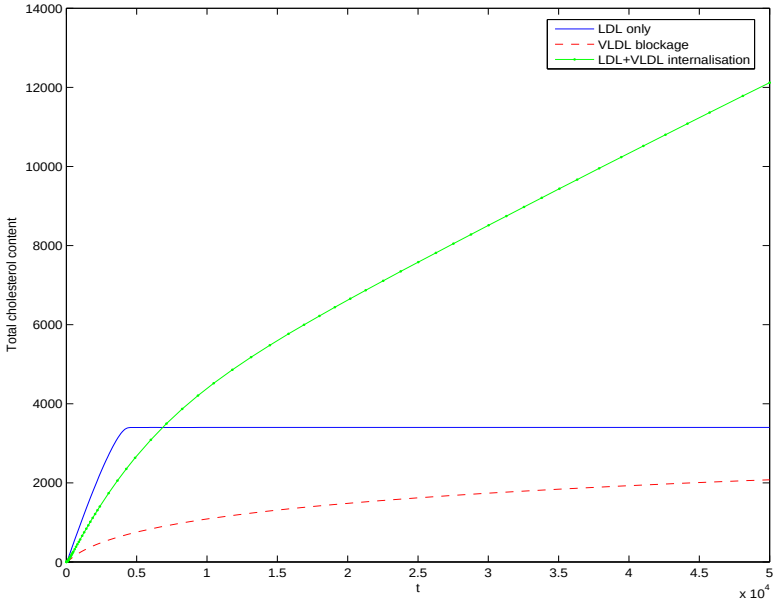

Figure 10: The same figure as per Figure 9(b), but over a longer time period showing the cholesterol content of the liver is highest for the case of LDL & VLDL internalisation. The cholesterol content for the VLDL blockage case tends to the same steady-state value when only LDL is present showing blockage only slows the amount of time taken for internalisation to occur. In each case $r = 2$, $\chi = 2.5 \times 10^{-3}$ and $\omega = 1$.

4 Conclusions and Future work

During the study group two models were formulated to consider the effect of LDL and VLDL binding and internalisation on the quantity of cholesterol in the liver. In the first instance we focused on LDL endocytosis in the absence of VLDL particles, and studied the effect of LDL binding, internalisation and degradation on the increase of extracellular cholesterol content. Our results suggest that the system's dynamics are most sensitive to changes in the rate at which pits are internalised, with intracellular cholesterol levels

increasing as pits are internalised more rapidly.

The second model included both the effects of LDL and VLDL binding and internalisation. Through model analysis we have been able to show that the rate of VLDL internalisation (of both type one and two) and receptor re-cycling is important in obtaining agreement with experimental data. However, whilst our results agree with current experimental data they predict that the overall cholesterol content of the liver for the three cases of LDL only binding and uptake, the blockage of LDL by VLDL and LDL & VLDL binding and internalisation will change with time; VLDL blockage only slows the rate of internalisation, hence given more time we expect the two curves to tend towards the same steady-state value as demonstrated in Figure 10. In the case of LDL & VLDL binding and internalisation the total cholesterol content of the liver will be higher than the previous two cases given the cholesterol content of each particle. We believe these differences would be observed if the experiments described in this report were undertaken for longer periods of time.

Future work in this area could include:

- testing the predictions of the second model regarding the total cholesterol content of the liver for long periods of time;
- understanding the effect that VLDL unbinding may have on the total cholesterol content;
- modifying the models to describe the way in which liver cells process LDL and VLDL in vivo (this would involve including source terms in the equations describing the evolution of extracellular LDL and VLDL);
- including more details regarding receptor recycling;
- combining the two models to obtain a more detailed description of pit and receptor dynamics.

5 Participants

The following people were involved with this problem during the study group: Nicola Armstrong, Leah Band, Helen Byrne, Kim Jackson, John King, Philip Murray, Brendan O'Malley, Jasmina Panovska, Laura Pickersgill, Johanna Stamper, Marcus Tindall, Jonathan Wattis and Christine Williams.

References

[1] M.S. Brown and J.L. Goldstein, *Receptor-mediated endocytosis: Insights from the lipoprotein receptor system*, Pro.Natl.Acad. Sci.USA, 76, 3330–3337, (1979).

[2] J.L. Goldstein, R.G.W. Anderson and M.S. Brown, *Coated pits, coated vesicles and receptor-mediated endocytosis*, Nature 279, 679–685, (1979).

[3] K.G. Jackson, C.M. Williams, B. O'Malley and L. Pickersgill, *Hepatic lipoprotein metabolism*, 5th Mathematics in Medicine Study Group, Oxford, September 2005.

[4] K.G. Jackson, V. Maitin, D.S. Leake, P. Yaqoob and C.M. Williams, *Saturated fat induced changes in Sf 60-400 particle composition reduces uptake of LDL by HepG2 cells*, Journal of Lipid Research, 47, 393-403, (2006).

[5] K.G. Jackson, E.J. Wolstencroft, P.A. Bateman, P. Yaqoob and C.M. Williams, *Greater enrichment of triacylglycerol-rich lipoproteins with apolipoproteins E and C-III after meals rich in saturated fatty acids than after meals rich in unsaturated fatty acids*, American Journal of Clinical Nutrition 81, 25–34, (2005).

[6] K.G. Jackson., *Personal Communication*, 24/11/2005.